iScience

CellPress
OPEN ACCESS

Article

ZIKV induces P62-mediated autophagic degradation of TRAF6 through TRAF6-NS1 interaction

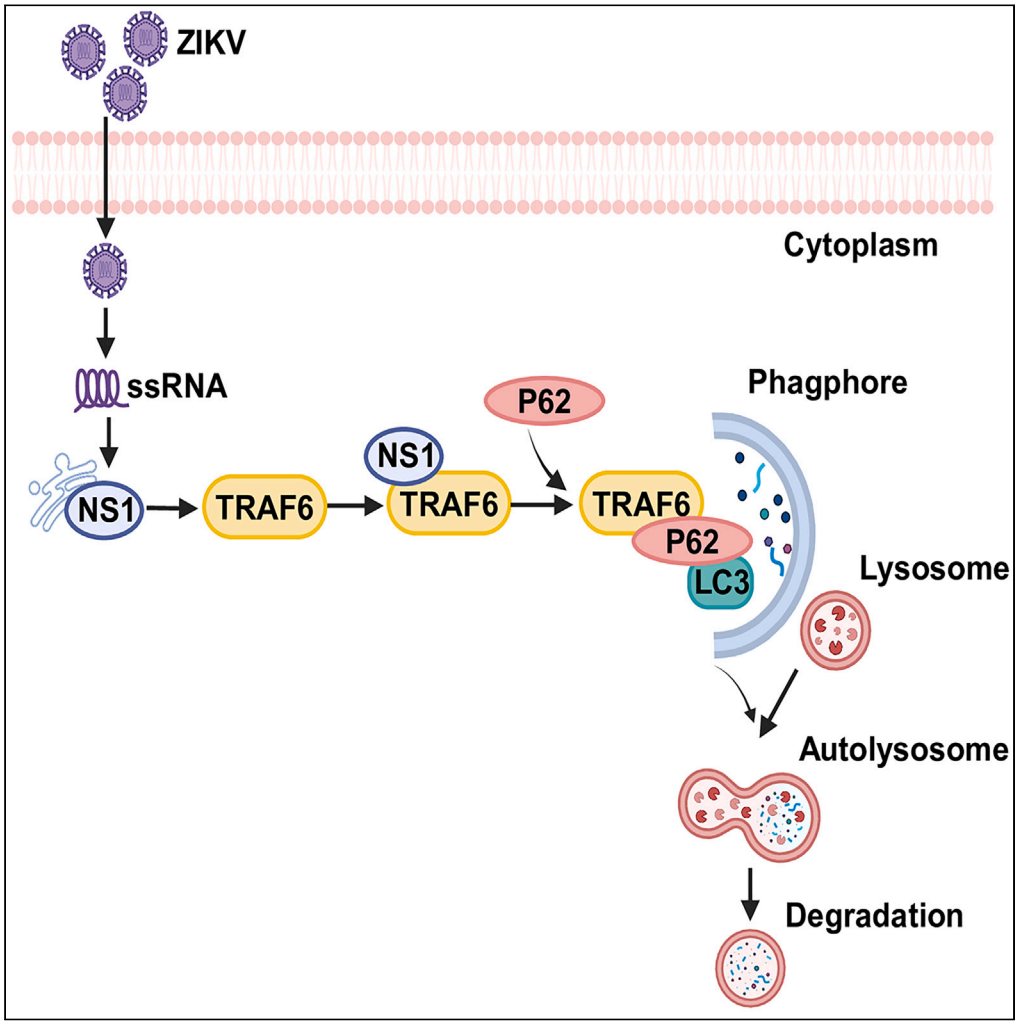

Shengze Zhang, Chuming Luo, Qiqi Chen, ..., Yuelong Shu, Nan Wu, Huanle Luo

shuylong@mail.sysu.edu.cn (Y.S.)
wnwunan@163.com (N.W.)
luohle@mail.sysu.edu.cn (H.L.)

Highlights

ZIKV inhibits TRAF6 expression both *in vitro* and *in vivo*

TRAF6's interaction with ZIKV NS1 induces P62-mediated autophagic degradation of TRAF6

TRAF6 promotes ZIKV infection

Zhang et al., iScience 27, 110757
September 20, 2024
https://doi.org/10.1016/j.isci.2024.110757

iScience

CellPress
OPEN ACCESS

Article

ZIKV induces P62-mediated autophagic degradation of TRAF6 through TRAF6-NS1 interaction

Shengze Zhang,[1,2,7] Chuming Luo,[1,2,7] Qiqi Chen,[1,2] Nina Li,[1,2] Xinzhong Liao,[1,2] Jiani Wu,[1,2] Haolu Zha,[1,2] Ting Xie,[1,2] Shaohui Bai,[1,2] Weijian Tian,[1,2] Lin Zhu,[1,2] Xuan Zou,[3] Shisong Fang,[3] Caijun Sun,[1,2,4] Ying Jiang,[5] Jianhui Yuan,[5] Yuelong Shu,[1,4,6,*] Nan Wu,[5,*] and Huanle Luo[1,2,4,8,*]

SUMMARY

Tumor necrosis factor receptor-associated factor 6 (TRAF6) is crucial in flavivirus infections, modulating the host immune response through interactions with viral proteins. Despite its importance, the relationship between TRAF6 and Zika virus (ZIKV) remains poorly understood. Our prior proteomics analysis revealed reduced TRAF6 protein levels in ZIKV-infected human trophoblast cells compared to non-infected controls. Subsequent studies in cell models and murine tissues confirmed a significant reduction in both TRAF6 mRNA and protein levels post-ZIKV infection. Further investigations unveiled that ZIKV induces P62-mediated degradation of TRAF6, with NS1 identified as the primary contributor. Co-localization and interaction studies demonstrated that NS1 promotes the association of P62, a key autophagy mediator, with TRAF6. Notably, our findings revealed TRAF6 enhances ZIKV infection, NS1 ubiquitination, NS1 expression, and the production of inflammatory cytokines and chemokines. These insights highlight the intricate TRAF6-ZIKV relationship, offering potential for drug targeting NS1-TRAF6 interactions to manage ZIKV infections effectively.

INTRODUCTION

Zika virus (ZIKV) belongs to the flavivirus family, which includes multiple pathogens transmitted by arthropod-borne vectors, such as Dengue virus (DENV) and West Nile virus (WNV). Similar to other flaviviruses, ZIKV encodes three structural proteins—capsid protein (C), pre-membrane (prM), and envelope protein (E)—along with seven nonstructural proteins (NS1, NS2A, NS2B, NS3, NS4A, NS4B, and NS5).[1] The nonstructural proteins primarily play roles in gene replication, translation, and regulation of the host immune response and metabolism, whereas the structural proteins are responsible for viral assembly and entry into host cells.[2,3] Despite its close genomic similarity to DENV and other flaviviruses, ZIKV infection poses serious health risks and is potentially linked to fetal neurodevelopmental defects, including fetal abortion and microcephaly, particularly when contracted during early pregnancy.[4,5] As of now, no vaccines or drugs have been developed for ZIKV infection, highlighting the urgency to study ZIKV pathogenesis and uncover possible mechanisms leading to disease.

One of the possible mechanisms for ZIKV pathogenesis is the inflammation caused in placental cells and neural cells. Tumor necrosis factor receptor-associated factor 6 (TRAF6) is a downstream adaptor of multiple inflammation related receptors, such as the TNFR superfamily, the toll-like receptor (TLR) family, interleukin-17 receptor (IL-17R), and interleukin-1 receptor (IL-1R).[6,7] It is abundantly expressed in various cells, particularly in macrophages, microglia, and neurons, mediating the host's inflammatory reactions. As an adaptor protein and E3 ubiquitin ligase, TRAF6 has been demonstrated to be associated with numerous brain-inflammatory-related diseases, such as ischemic stroke and Parkinson's disease.[8,9] Previous reports have demonstrated that prototypical RNA viruses exhibit enhanced replication and increased cytopathicity in TRAF6-deficient cells due to a dampened interferon (IFN) response.[7,10] Importantly, the TRAF6 signaling pathway assumes distinct roles in flavivirus infections. It facilitates Langat virus (LGTV) replication by binding to the viral non-structural protein NS3, while it inhibits WNV replication in mouse embryonic fibroblasts (MEF).[11] DENV and Japanese encephalitis virus (JEV) have been observed to up-regulate cellular miR-146a, resulting in the downregulation of TRAF6 expression and signaling. This suppression of TRAF6, in turn, leads to a decreased activation of multiple cytokines.[12,13] Additionally, in the case of DENV, the downregulation of TRAF6 also inhibits virus-induced autophagy.[14]

[1]School of Public Health (Shenzhen), Shenzhen Key Laboratory of Pathogenic Microbes and Biosafety, Shenzhen Campus of Sun Yat-sen University, Shenzhen 518107, P.R. China
[2]School of Public Health (Shenzhen), Sun Yat-sen University, Guangzhou 510275, P.R. China
[3]Shenzhen Center for Disease Control and Prevention, Shenzhen 518073, P.R. China
[4]Key Laboratory of Tropical Disease Control (Sun Yat-sen University), Ministry of Education, Guangzhou 510080, P.R. China
[5]Shenzhen Nanshan Center for Disease Control and Prevention, Shenzhen 518054, P.R. China
[6]Key Laboratory of Pathogen Infection Prevention and Control (MOE), State Key Laboratory of Respiratory Health and Multimorbidity, National Institute of Pathogen Biology, Chinese Academy of Medical Sciences & Peking Union Medical College, Beijing 102629, P.R. China
[7]These authors contributed equally
[8]Lead contact
*Correspondence: shuylong@mail.sysu.edu.cn (Y.S.), wnwunan@163.com (N.W.), luohle@mail.sysu.edu.cn (H.L.)
https://doi.org/10.1016/j.isci.2024.110757

Nevertheless, the presence of TRAF6 in the newly emerging ZIKV, a flavivirus, is limited. A study suggests that treating HMC3 cells with the NS1 protein of ZIKV suppresses the expression of TRAF6 and related antiviral responses.[15] However, whether ZIKV infection affects TRAF6 and the underlying mechanism is not investigated in detail.

In this study, we observed a significant decrease in both TRAF6 mRNA and protein levels *in vitro* and various tissues of mice compared to non-infected controls. Subsequent findings indicated that ZIKV not only inhibits TRAF6 expression but also facilitates its degradation through P62-mediated autophagy. Further investigation unveiled an interaction between the NS1 protein of ZIKV and TRAF6, enhancing the association between P62 and TRAF6. Our study also revealed that TRAF6 facilitates ZIKV infection, protein synthesis, and the production of pro-inflammatory cytokines. Overall, the identified TRAF6-NS1 interaction not only enhances our understanding of ZIKV infection mechanisms but also presents a promising avenue for developing targeted interventions to control this viral threat.

RESULTS

ZIKV infection leads to reduced TRAF6 expression both *in vitro* and *in vivo*

In our previous proteomics studies, we observed a decrease in TRAF6 protein level in ZIKV-infected trophoblast cells (HTR8) compared to non-infected controls (Figure S1A). To validate this finding, we conducted quantitative polymerase chain reaction (qPCR) and Western blot analyses in both HTR8 and human glioblastoma cells (U251). The results indicated a significant decrease in *TRAF6* mRNA levels on day 2 and day 4 in both ZIKV-infected HTR8 and U251 cells, as compared to the non-infected group (Figures 1A and 1C). Consistently, a reduction in TRAF6 protein levels was observed at 12, 24, 36 and 48 h post-infection in ZIKV-infected HTR8 cells, and at 24, 36 and 48 h post-infection in ZIKV-infected U251 cells, when compared to the non-infected controls. (Figures 1B and 1D). Additionally, we observed a decrease in TRAF6 mRNA levels in various tissues of ZIKV-infected mice on days 2 and 6, including blood cells, spleen, brain, testis, and uterus, in comparison to the non-infected group (Figures 1E–1I). Correspondingly, TRAF6 protein levels decreased in the spleen (Figures 1J and S2A) and uterus (Figures 1L and S2C) on both day 2 and day 6, and in the brain on day 6 (Figures 1K and S2B), with no significant differences observed in the testis (data not shown) following ZIKV infection. These results suggest that ZIKV infection decreases TRAF6 expression both in *in vitro* models and in multiple tissues *in vivo*.

ZIKV infection promotes TRAF6 degradation through P62-mediated autophagy

Subsequently, we used cycloheximide (CHX) to inhibit protein synthesis and explored the impact of ZIKV on TRAF6 degradation in U251 cells. Our observations revealed persistent reductions in TRAF6 protein levels at 0, 6, 12 and 24 h of post-CHX treatment following ZIKV infection for 24 h compared to non-infected groups (Figures 2A and S3A), suggesting that ZIKV induces TRAF6 degradation rather than merely inhibiting its synthesis. To elucidate the mechanism underlying ZIKV-induced TRAF6 degradation, we employed various inhibitors, including MG132 for the proteasome degradation, 3-MA for autophagy by blocking autophagosome formation in the earlier stage, Chloroquine (CQ) for autophagy by impairing autophagosome fusion with lysosome in the later stage, and Z-FA-FMK as a pan-caspase inhibitor.[16,17] As depicted in the Figures 2B and S3B, our findings indicate that CQ effectively prevented the degradation induced by ZIKV. This suggests that ZIKV infection degrades TRAF6 through the autophagy pathway. This suggests that ZIKV infection degrades TRAF6 through the autophagy pathway. Indeed, ZIKV infection activates autophagy, as evidenced by the degradation of P62 and the conversion of LC3B I to LC3B II, as observed in the Figures 2C and S3C. Subsequently, upon performing a knockdown of P62 through siRNA transfection,[18] we observed the inhibition of TRAF6 degradation and less conversion of LC3B I to LC3B II caused by ZIKV at both 24 and 48 h post-infection (Figures 2D and S3D). These results strongly indicate that ZIKV infection degrades TRAF6 via the involvement of P62-mediated autophagy.

The degradation of TRAF6 is attributed to the NS1 protein of ZIKV

We further investigated the nonstructural proteins encoded by ZIKV responsible for TRAF6 degradation by measuring TRAF6 expression after overexpressing 0.5 μg or 1 μg of NS1, NS2A, NS2B, NS3, NS4A, NS4B, or NS5. As depicted in Figures 3A and S4A–S4F, the overexpression of NS1 significantly inhibits TRAF6 expression in a dose-dependent manner. We also observed that NS1 overexpression continues to reduce TRAF6 even with CHX treatment, suggesting that NS1 can degrade TRAF6 (Figures 3B and S5A). Furthermore, treatment with CQ can rescue this degradation, further indicating that NS1 is responsible for the degradation induced by ZIKV infection (Figures 3C and S5B). We also noted that NS1 degrades P62 and promotes the conversion of LC3B I to LC3B II (Figures 3D and S5C). However, this conversion, along with TRAF6 degradation, was reversed by the knockdown of p62 (Figures 3E and S5D). These findings suggest that NS1 induces TRAF6 degradation via p62-mediated autophagy.

Furthermore, we observed colocalization of NS1 with TRAF6 in both U251 cells and 293T cells (Figures 4A and 4B). NS1 demonstrated interaction with endogenous TRAF6 in U251 cells and with exogenous TRAF6 in 293T cells (Figures 4C–4F). Motivated by a prior report suggesting the interaction between P62 and TRAF6.[19] we investigated the interaction between NS1, P62, and TRAF6. Interestingly, our findings revealed an enhanced pull-down of P62 with NS1 expression compared to the control (Figure 4G). These results suggest that NS1 encoded by ZIKV has the capability to promote the degradation of TRAF6 by enhancing the interaction between TRAF6 and P62.

TRAF6 facilitates ZIKV infection *in vitro*

As NS1 interacts with TRAF6, we sought to elucidate the role of TRAF6 during ZIKV infection. To investigate this, we conducted siRNA knockdown experiments, achieving a reduction of at least 50% in both mRNA and protein levels (Figures S6A and S6B) in U251 cells, which

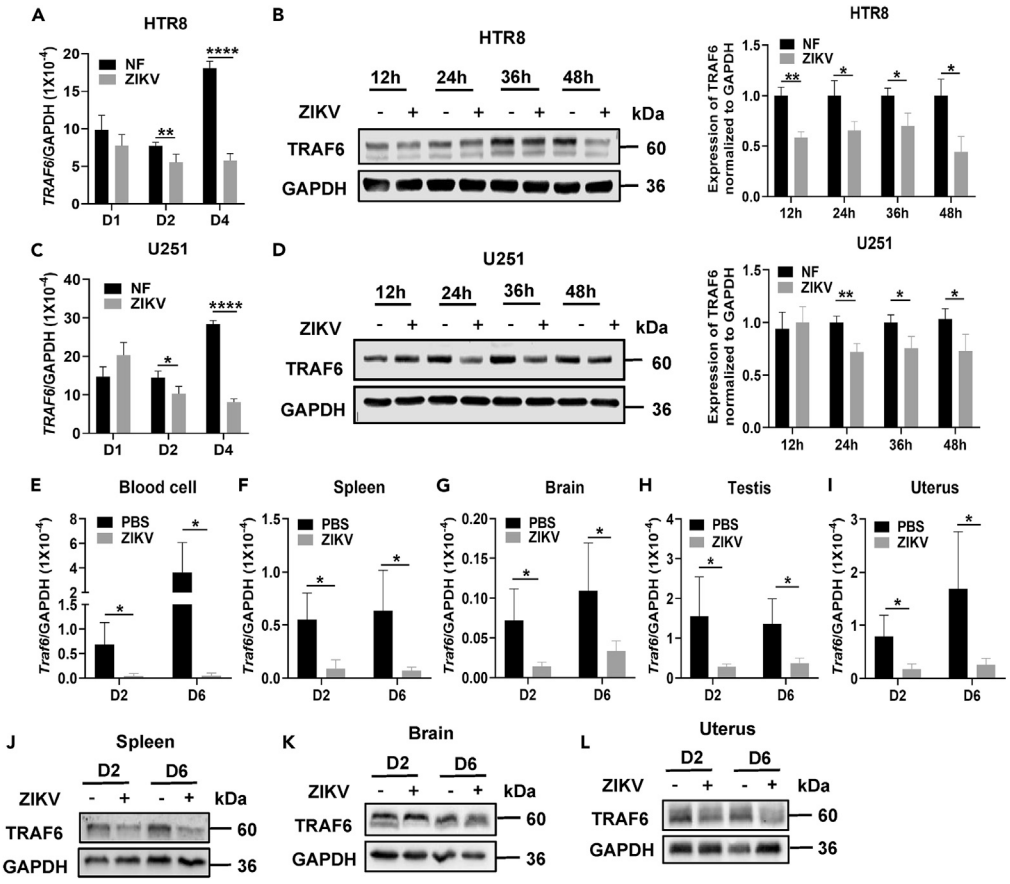

Figure 1. TRAF6 expression in HTR8 cells, U251 cells, and murine tissues post-ZIKV infection

(A) HTR8 cells were infected with ZIKV at an MOI of 1. mRNA levels of TRAF6 were measured on day 1 (D1), D2 and D4 post-infection by qPCR.

(B) Western blot assay (left panel) of TRAF6 expression in HTR8 cells infected with ZIKV for 12 h (h), 24h, 36h and 48h. Quantification (right panel) of TRAF6 protein levels relatives to GAPDH.

(C) U251 cells were infected with ZIKV at an MOI of 1. mRNA levels of TRAF6 were measured on D1, D2 and D4 post-infection by qPCR.

(D) Western blot assay (left panel) of TRAF6 expression in U251 cells infected with ZIKV for 12h, 24h, 36h and 48h. Quantification (right panel) of TRAF6 protein levels relatives to GAPDH.

(E–I) 6-8-week-old mice were treated with 2 mg MAR1-5A3 on the day prior to infection and then i.p. inoculated with 5×10^4 PFU of ZIKV. mRNA levels of TRAF6 in blood cells (E), spleen (F), brain (G), testis (H) and uterus (I) were measured on D2 and D6 post-infection by qPCR. There were 4 mice per group.

(J–L) Western blot assay of TRAF6 expression in ZIKV-infected spleen (J), brain (L) and uterus (L). The data represent a single experiment chosen as representative from three independent experiments. All the data are analyzed by unpaired Student's *t* test. Data are presented as means ± SD. $*p < 0.05$, $**p < 0.01$, $****p < 0.0001$ compared to control group.

See also Figures S1 and S2.

were subsequently infected with ZIKV. Viral loads in TRAF6 siRNA-transfected[20] U251 cells showed a significant decrease on days 1, 2, and 3 post-infection when compared to control siRNA-treated cells, as assessed by qPCR and plaque assay (Figures 5A and 5B). Additionally, we observed a reduction in NS5 expression at 36 and 48 h with the knockdown of TRAF6 post-infection (Figure 5C). These results suggest that TRAF6 promotes ZIKV infection in U251 cells. Considering TRAF6's role as an E3 ligase.[21] we utilized C25-140, a TRAF6 inhibitor, to impede the interaction between TRAF6 and E2 ligase. This approach was taken to investigate whether the ubiquitination process is involved. As a result, we observed reduced mRNA levels on day 2 post-infection and decreased viral titers on both day 1 and day 2 post-infection (Figures 5D and 5E).

We then investigated whether the interaction between TRAF6 and NS1 affects NS1 ubiquitination. As depicted in Figures 5F and 5G, we observed ubiquitination of NS1 at both K48 and K63 in 293T cells transfected with NS1. Furthermore, the addition of TRAF6 enhanced the K63 ubiquitination (Figures 5H and S7A) rather than the K48 ubiquitination of NS1 (Figures 5I and S7B). These results indicate that TRAF6 mediates the K63 ubiquitination of NS1. To further investigate the relationship between NS1 and TRAF6, we overexpressed NS1 in 293T cells transfected with TRAF6 siRNA. We observed a decrease in NS1 levels at 24 and 48 h post-transfection compared to the controls (Figure 5J). Conversely, the overexpression of TRAF6 resulted in a dose-dependent increase in NS1 expression (Figure 5K). These results indicate that TRAF6 promotes ZIKV infection and protein synthesis in U251 cells, and the E3 ligase activity is involved.

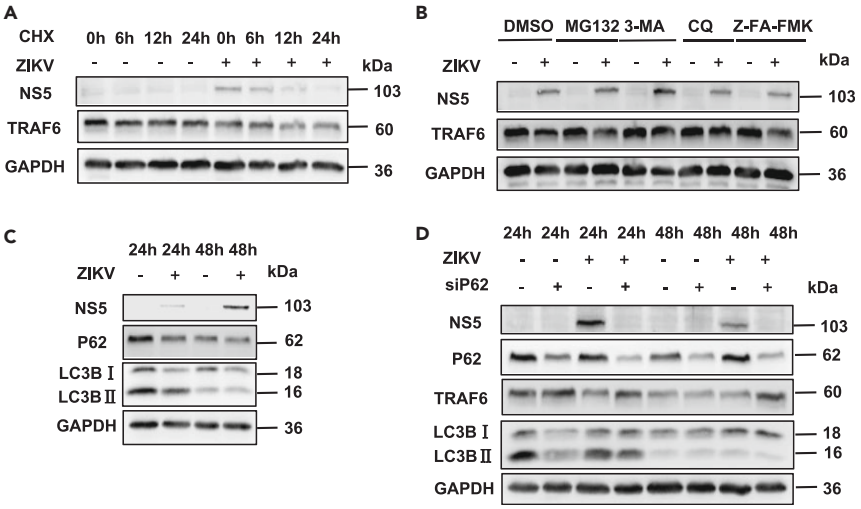

Figure 2. ZIKV infection induces TRAF6 autophagic degradation mediated by P62

(A) U251 cells, infected with ZIKV at an MOI of 1 for 24h, were subsequently treated with cycloheximide (CHX, 30 μg/mL). TRAF6 expression was evaluated by western blot at 0h, 6h, 12h, and 24h of CHX treatment.

(B) U251 cells were infected with ZIKV for 24 h at an MOI of 1, followed by treatment with DMSO, proteasome inhibitor MG132 (20 μM), autophagosome inhibitor 3-MA (1 mg/mL), lysosome inhibitor CQ (100 μM) or apoptosis inhibitor Z-FA-FMK (50 μM) for 4h. TRAF6 expression was assessed by western blot.

(C) Western blot assays of P62 and LC3 expression in U251 cells infected with ZIKV for 24h and 48h.

(D) U251 cells were infected with ZIKV at an MOI of 1 post siP62 transfection. At 24h and 48h post-infection, TRAF6, P62 and LC3 levels were measured by western blot. The data represent a single experiment chosen as representative from three independent experiments.

See also Figure S3.

TRAF6 positively regulates ZIKV-induced inflammation

TRAF6 has been identified as a downstream adaptor of multiple receptor families related to inflammation. To assess the impact of TRAF6 on ZIKV-induced inflammatory responses, we compared the levels of inflammatory cytokines and chemokines between TRAF6 knockdown cells and the control group. As illustrated in Figures 6A–6E, pro-inflammatory cytokines including IL-1α, IL-6, IL-16, IL-17A and TNFα were induced upon ZIKV infection at 24 h post-infection. However, with the knockdown of TRAF6, these inflammatory cytokines exhibited a decrease. Furthermore, we observed a significant increase in CCL5 at 48 h and CXCL10 at both 24 and 48 h in ZIKV-infected cells. The deficiency of TRAF6 reversed this elevation, as illustrated in Figures 6F and 6G. These results suggest that ZIKV induces these cytokines through the TRAF6 signaling pathway. In contrast, for interferons, we noted a decrease in IFNγ mRNA levels but an induction of IFNβ mRNA levels during ZIKV infection. This effect was reversed by TRAF6 (Figures 6H and 6I). Overall, these results demonstrate that TRAF6 influences ZIKV-induced cytokines, including inflammatory cytokines, chemokines, and interferons.

DISCUSSION

The balance in host-viral interactions plays a pivotal role in viral pathogenesis. Viruses employ strategically encoded proteins to interact with key checkpoints in the immune response, thereby modulating antiviral processes. In our study, we uncovered that NS1, encoded by ZIKV, not only suppresses the expression of TRAF6 but also facilitates its degradation through P62-mediated autophagy. This discovery offers valuable insights into comprehending the pathogenesis of ZIKV.

Numerous non-structural proteins encoded by ZIKV interact with host factors to enhance its infection. Specifically, NS1 and NS4B exhibit the capability to inhibit IFN by interacting with TANK-binding kinase 1 (TBK1).[22] NS1 also can inhibit the proteasomal degradation of caspase 1, which initiates type I IFN signaling during ZIKV infection.[23] Moreover, the interaction between NS2B-NS3 of ZIKV and Janus Kinase 1 (JAK1) leads to the degradation of JAK1, highlighting the virus's multifaceted strategies to subvert host immune responses.[24] However, limited studies about the interaction between ZIKV and TRAF6, which serves as a crucial bridge between innate and adaptive immunity, and its dysregulation may have significant implications for the host's antiviral defenses.[25] As we also observed the inhibition of TRAF6 transcription, we believe that the decrease of TRAF6 results from both degradation and reduced synthesis. While we have explored the mechanism for TRAF6 degradation, the mechanism for the inhibition of TRAF6 synthesis remains unknown. A previous study demonstrated that exposure of human microglial cells to ZIKV-NS1 resulted in an increased expression of miR-146a. This upregulation, in turn, led to the suppression of TRAF6 expression and its associated signaling pathways.[15] We speculate that miR-146a may also be involved in the inhibition of TRAF6 synthesis and will investigate this further. These findings suggest an indirect mechanism by which NS1 suppresses TRAF6 expression, implying that ZIKV may regulate TRAF6 indirectly. In our study, we further elucidate this process by demonstrating that NS1 directly interacts with TRAF6, promoting TRAF6 degradation through P62-mediated autophagy. Collectively, these studies suggest a crucial role for TRAF6 in ZIKV infection, although no prior studies have explicitly illustrated this.

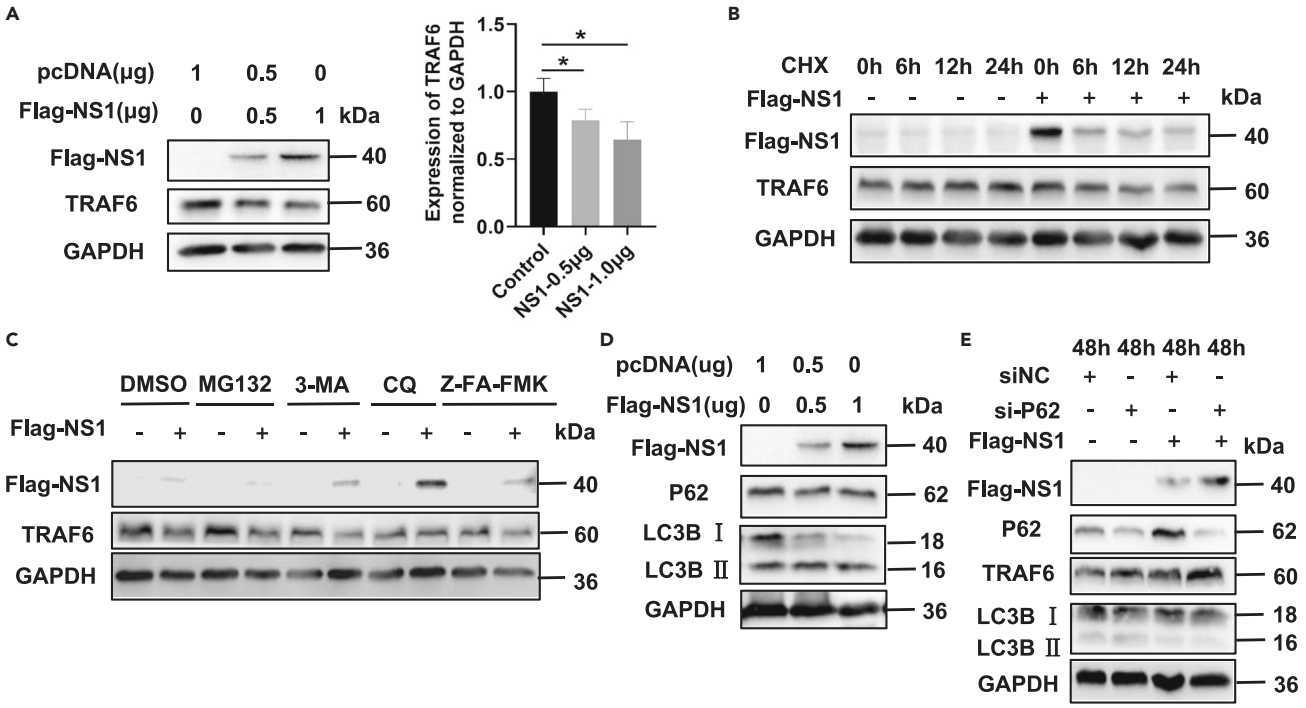

Figure 3. NS1 promotes a P62-mediated autophagic degradation

(A) U251 cells were transfected with pcDNA or Flag-NS1 plasmid at 0, 0.5 or 1 μg for 24h. TRAF6 expression was assessed by western blot (left panel). Quantification (right panel) of TRAF6 protein levels relatives to GAPDH was measured. The data represent the collective results of three independent experiments.

(B) U251 cells were transfected with pcDNA or Flag-NS1 plasmid (1 μg) for 24h followed by treatment with CHX (30 μg/mL). TRAF6 expression was assessed by western blot after being treated with CHX for 0h, 6h, 12h and 24h.

(C) U251 cells were transfected with pcDNA or Flag-NS1 (1 μg) plasmid for 24h followed by treatment with DMSO, proteasome inhibitor MG132 (20 μM), autophagosome inhibitor 3-MA (1 mg/mL), lysosome inhibitor CQ (100 μM) or apoptosis inhibitor Z-FA-FMK (50 μM) for 4h. TRAF6 expression was assessed by western blot.

(D) Western blot assays of P62 and LC3 expression in U251 cells transfected with pcDNA or Flag-NS1 plasmid at 0, 0.5 or 1 μg for 24h.

(E) U251 cells were transfected with pcDNA or Flag-NS1 (1 μg) plasmid post siP62 transfection. At 24h post-transfection, TRAF6, P62 and LC3 levels were measured by western blot. The data represent a single experiment chosen as representative from three independent experiments. Data are presented as means ± SD. *$p < 0.05$, **$p < 0.01$ compared to control group.

See also Figure S4.

While prior studies have delineated the dual role of TRAF6 in flavivirus infections inhibiting mosquito-borne viruses like WNV and Kunjin virus but promoting replication of tick-borne flaviviruses through NS3 interaction,[11] our investigation introduces a novel perspective. In U251 cells, TRAF6 surprisingly promotes ZIKV infection, a phenomenon occurring alongside ZIKV-induced down-regulation of TRAF6. This nuanced dynamic underscores the critical role of TRAF6 in navigating the complex interplay between the virus and the host immune response. Our findings with TRAF6 deficiency yield significant insights. Notably, we observe a reduction in IFNβ mRNA levels in ZIKV-infected U251 cells lacking TRAF6, a phenomenon typically associated with inhibitory effects on ZIKV infection.[24,26,27] Furthermore, our study uncovers TRAF6's involvement in diminishing IFNγ production, which plays a unique and promoting role in ZIKV infection.[28] Additionally, a substantial decrease is noted in several NF-κB-related cytokines (IL-1α, IL-6, TNFα, and CCL5) in ZIKV-infected U251 cells with TRAF6 deficiency. These cytokines, integral to the inflammatory response, are closely intertwined with ZIKV infection.[29,30] Our study, thus, provides a comprehensive view of the intricate regulatory role played by TRAF6 in ZIKV infection dynamics.

One limitation of our study is the unexplored mechanism through which TRAF6 promotes NS1 expression *in vitro*. We hypothesize that K63 ubiquitination of NS1 by TRAF6 may play a crucial role in this process. Previous studies have shown that K27 ubiquitination of DENV NS3 can enhance the formation of the NS2B3 protease complex, consequently boosting viral replication.[31] However, additional studies are necessary to delve into the underlying mechanism. As several small molecule inhibitors have been developed to inhibit TRAF6 signaling, targeting TRAF6 expression *in vivo* might be a potential strategy to protect mice from ZIKV infection, given that we have found TRAF6 facilitates ZIKV infection *in vitro*.

In summary, our study has illustrated that ZIKV NS1 has the capability to suppress TRAF6 expression and facilitate TRAF6 degradation through P62-mediated autophagy. This discovery unveils a mechanism by which ZIKV exploits critical host factors to modulate the immune system, ultimately for its benefit in evading the immune system.

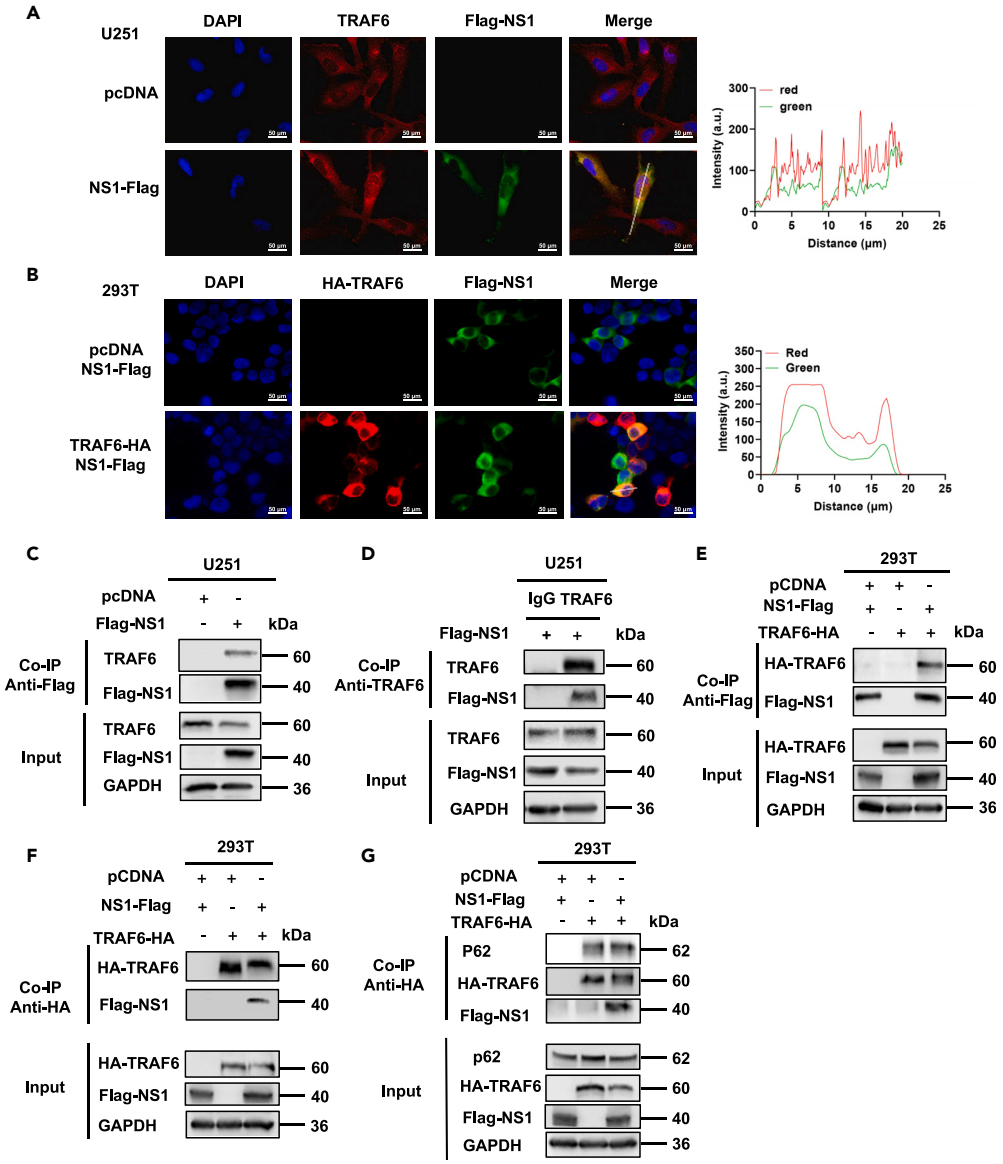

Figure 4. Interaction between NS1 and TRAF6 in U251 cells and 293T cells

(A) U251 cells transfected with pcDNA or Flag-NS1 (0.5 μg) plasmid for 24h were analyzed by confocal microscopy (left panel). Cell nuclei were stained using DAPI (blue). Endogenous TRAF6 was labeled with anti-TRAF6 antibody (red). Flag-NS1 was labeled with anti-Flag antibody (green). Scale bar = 50 μm. The intensity plot of region of interest (straight white line) was shown in right panel. Red curves show the relative intensity of endogenous TRAF6, green curves show the relative intensity of Flag-NS1.

(B) 293T cells co-transfected with Flag-NS1 (0.5 μg) and HA-TRAF6 plasmids for 24h were analyzed by confocal microscopy (left panel). Cell nuclei were stained using DAPI (blue). HA-TRAF6 was labeled with anti-HA antibody (red). Flag-NS1 was labeled with anti-Flag antibody (green). Scale bar = 50 μm. The intensity plot of region of interest (straight white line) was shown in right panel. Red curves show the relative intensity of HA-TRAF6, green curves show the relative intensity of Flag-NS1.

(C and D) U251 cells were transfected with pcDNA or Flag-NS1 (5 μg) plasmid for 24h. Cellular lysates were subjected to immunoprecipitation with anti-Flag magnetic beads, anti-IgG agarose beads or anti-TRAF6 agarose beads and western blot assays using the indicated antibodies.

(E–G) 293T cells were co-transfected with HA-TRAF6 (5 μg) and Flag-NS1 (5 μg) plasmid for 48h. Cellular lysates were subjected to immunoprecipitation with anti-Flag or anti-HA magnetic beads and western blot assays using the indicated antibodies. The data represent a single experiment chosen as representative from three independent experiments.

Limitations of the study

In this study, we showed that ZIKV NS1 facilitates TRAF6 degradation through P62-mediated autophagy. However, the roles of TRAF6 during ZIKV infection should be investigated further in animal models.

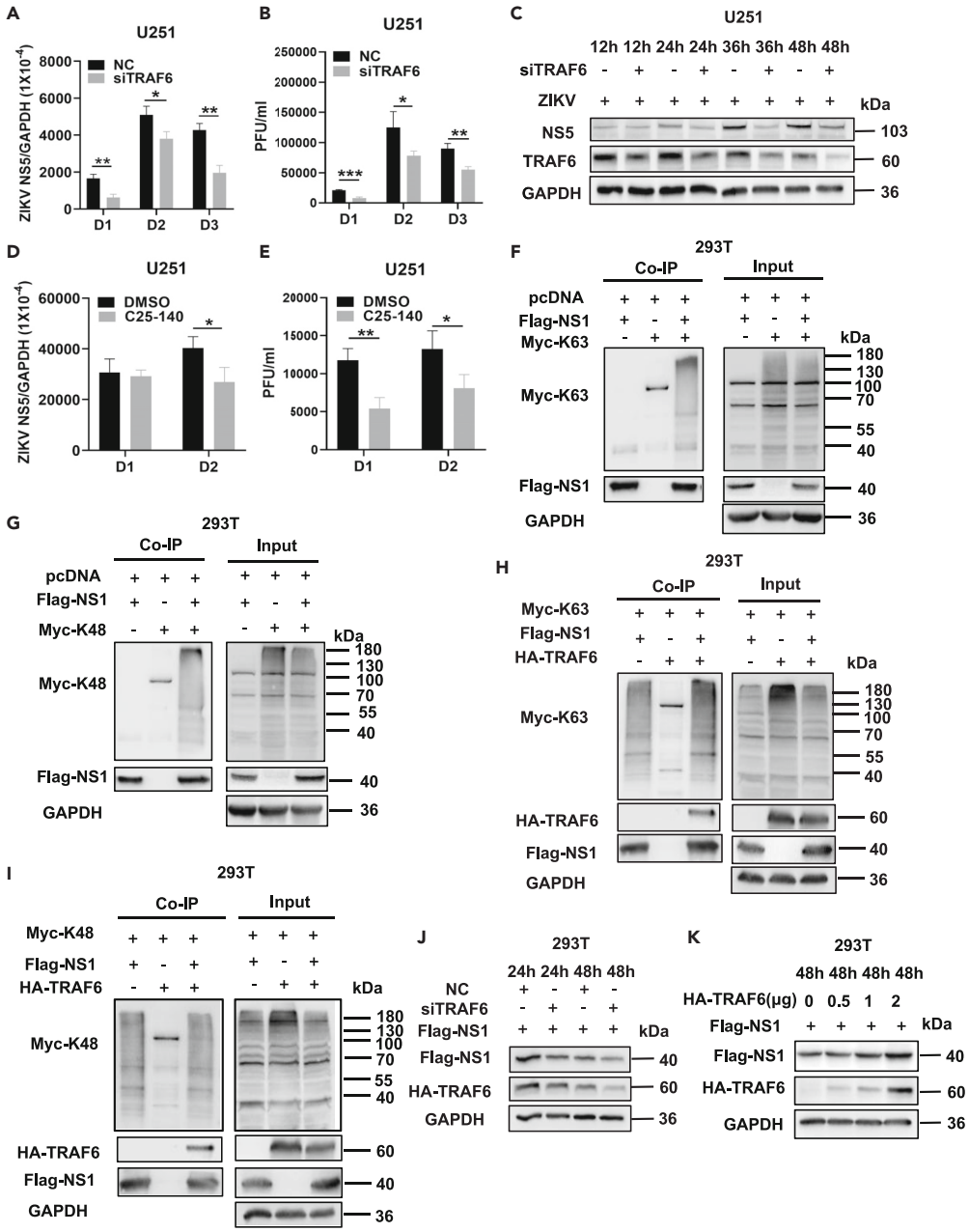

Figure 5. TRAF6 enhance the expression and K63 ubiquitination of NS1

(A and B) U251 cells were infected with ZIKV at an MOI of 1 following negative control (NC) siRNA or TRAF6 siRNA transfection for 24h. The ZIKV NS5 mRNA levels were measured on D1, D2 and D3 post-infection by qPCR and by plaque assay (B).

(C) Western blot assays of ZIKV NS5 and TRAF6 expression in U251 cells post TRAF6 siRNA transfection and infected with ZIKV for 12h, 24h, 36h and 48h.

(D and E) U251 cells were infected with ZIKV at an MOI of 1 for 1h followed by treatment with DMSO or C25-140 (20mM). The viral load was measured on D1, D2 and D4 post-infection by qPCR (C) and plaque assay (D).

(F and G) 293T cells were co-transfected with Myc-K63 (5 μg) plasmid (F) or Myc-K48 (5 μg) plasmid (G) and Flag-NS1 (5 μg) plasmid for 48h. Cellular lysates were subjected to immunoprecipitation with anti-Flag magnetic beads and western blot assays using the indicated antibodies.

(H and I) 293T cells were co-transfected with Myc-K63 (5 μg) plasmid (H) or Myc-K48 (5 μg) plasmid (I), Flag-NS1 (5 μg) plasmid and HA-TRAF6 (5 μg) plasmid for 48h. Cellular lysates were subjected to immunoprecipitation with anti-Flag magnetic beads and western blot assays using the indicated antibodies.

(J) U251 cells were transfected with Flag-NS1 (1 μg) plasmid post TRAF6 siRNA transfection for 24h. NS1 and TRAF6 expression were assessed at 24h and 48h post-transfection by western blot.

Figure 5. *Continued*

(K) Western blot assays of Flag-NS1 and HA-TRAF6 expression in U251 cells post HA-TRAF6 (0, 0.5, 1, 2 μg) and Flag-NS1 (1 μg) plasmids co-transfection for 48h. The data represent a single experiment chosen as representative from three independent experiments. All the data are analyzed by unpaired Student's *t* test. Data are presented as means ± SD. *$p < 0.05$, **$p < 0.01$ compared to control group.

See also Figures S6 and S7.

RESOURCE AVAILABILITY

Lead contact

Further information and requests for resources and reagents should be directed to and will be fulfilled by the lead contact, H.L. (luohle@mail.sysu.edu.cn).

Materials availability

This study did not generate new unique reagents. All unique/stable reagents used in this study are available from the lead contact with a completed Materials Transfer Agreement.

Data and code availability

This paper does not report original code.

All data reported in this paper will be shared by the lead contact upon request.

Any additional information required to reanalyze the data reported in this paper is available from the lead contact upon request.

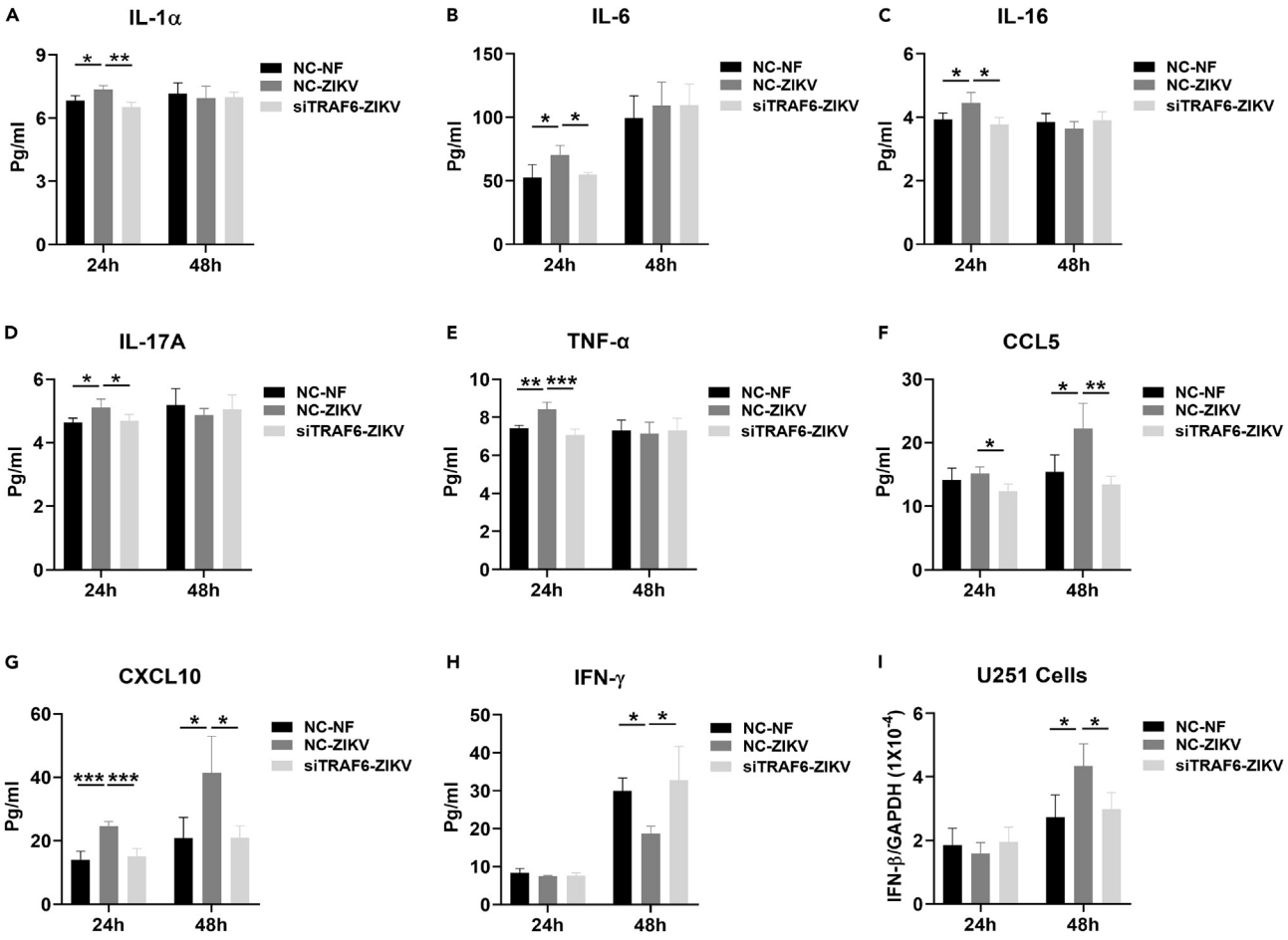

Figure 6. TRAF6 affects ZIKV-induced inflammatory cytokine production in U251 cells

(A–I) U251 cells were infected with ZIKV at an MOI of 1 following the NC or TRAF6 siRNA transfection for 24h. Cytokine levels in the supernatant including NF group, infected group and knock-down TRAF6 with ZIKV infection group were measured by bioplex (A–H), and IFNβ mRNA levels were measured by qPCR at 24h and 48h post-infection (I). Data are collected from 4 samples per group and analyzed by unpaired Student's *t* test. Data are presented as means ± SD. *$p < 0.05$, **$p < 0.01$, ***$p < 0.001$ compared to control group.

ACKNOWLEDGMENTS

This work was supported by National Natural Science Foundation of China (32000116, 32270147), Shenzhen Science and Technology Program (KQTD20200820145822023, JCYJ20190807155407443, KCXFZ20211020172545006, ZDSYS20230626091203007), High-Level Project of Medicine in Nanshan, Shenzhen; Sanming Project of Medicine in Shenzhen (SZSM202103008), Science and Technology Planning Project of Guangdong Province China (2021B1212040017).

AUTHOR CONTRIBUTIONS

H.L. and S.Z. conceptualized the study and designed the experiments. S.Z. conducted most of the experiments. C.L., Q.C., N.L., X.L., J.W., H.Z., T.X., S.B., W.T., L.Z., X.Z., and S.F. assisted with experiments. C.S., Y.J., J.Y., Y.S., N.W., and H.L. generated resources. H.L., S.Z., C.L., Q.C., N.W., and Y.S. contributed to data analyses and manuscript writing.

DECLARATION OF INTERESTS

The authors declare no competing interests.

STAR★METHODS

Detailed methods are provided in the online version of this paper and include the following:

- KEY RESOURCES TABLE
- EXPERIMENTAL MODEL AND STUDY PARTICIPANT DETAILS
  - Animal experiments
  - Cell culture and virus
- METHOD DETAILS
  - Viral infection
  - Proteomic analysis
  - Quantitative real-time PCR (qPCR)
  - Western blot
  - Immunofluorescence assay
  - Co-immunoprecipitation (Co-IP)
  - Cytokine Bio-Plex assay
- QUANTIFICATION AND STATISTICAL ANALYSIS

SUPPLEMENTAL INFORMATION

Supplemental information can be found online at https://doi.org/10.1016/j.isci.2024.110757.

Received: February 17, 2024
Revised: June 7, 2024
Accepted: August 14, 2024
Published: August 20, 2024

REFERENCES

1. Hasan, S.S., Sevvana, M., Kuhn, R.J., and Rossmann, M.G. (2018). Structural biology of Zika virus and other flaviviruses. Nat. Struct. Mol. Biol. *25*, 13–20. https://doi.org/10.1038/s41594-017-0010-8.
2. Guo, M., Hui, L., Nie, Y., Tefsen, B., and Wu, Y. (2021). ZIKV viral proteins and their roles in virus-host interactions. Sci. China Life Sci. *64*, 709–719. https://doi.org/10.1007/s11427-020-1818-4.
3. Ci, Y., Liu, Z.-Y., Zhang, N.-N., Niu, Y., Yang, Y., Xu, C., Yang, W., Qin, C.-F., and Shi, L. (2020). Zika NS1–induced ER remodeling is essential for viral replication. J. Cell Biol. *219*, e201903062. https://doi.org/10.1083/jcb.201903062.
4. Parra, B., Lizarazo, J., Jiménez-Arango, J.A., Zea-Vera, A.F., González-Manrique, G., Vargas, J., Angarita, J.A., Zuñiga, G., Lopez-Gonzalez, R., Beltran, C.L., et al. (2016). Guillain-Barré Syndrome Associated with Zika Virus Infection in Colombia. N. Engl. J. Med. *375*, 1513–1523. https://doi.org/10.1056/NEJMoa1605564.
5. de Araújo, T.V.B., Rodrigues, L.C., de Alencar Ximenes, R.A., de Barros Miranda-Filho, D., Montarroyos, U.R., de Melo, A.P.L., Valongueiro, S., de Albuquerque, M.d.F.P.M., Souza, W.V., Braga, C., et al. (2016). Association between Zika virus infection and microcephaly in Brazil, January to May, 2016: preliminary report of a case-control study. Lancet Infect. Dis. *16*, 1356–1363. https://doi.org/10.1016/s1473-3099(16)30318-8.
6. Inoue, J.-I., Gohda, J., and Akiyama, T. (2007). Characteristics and Biological Functions of TRAF6. In TNF Receptor Associated Factors (TRAFs), H. Wu, ed. (Springer), pp. 72–79. https://doi.org/10.1007/978-0-387-70630-6_6.
7. Yoshida, R., Takaesu, G., Yoshida, H., Okamoto, F., Yoshioka, T., Choi, Y., Akira, S., Kawai, T., Yoshimura, A., and Kobayashi, T. (2008). TRAF6 and MEKK1 Play a Pivotal Role in the RIG-I-like Helicase Antiviral Pathway. J. Biol. Chem. *283*, 36211–36220. https://doi.org/10.1074/jbc.M806576200.
8. Lalani, A.I., Zhu, S., Gokhale, S., Jin, J., and Xie, P. (2018). TRAF molecules in inflammation and inflammatory diseases. Curr. Pharmacol. Rep. *4*, 64–90. https://doi.org/10.1007/s40495-017-0117-y.
9. Dou, Y., Tian, X., Zhang, J., Wang, Z., and Chen, G. (2018). Roles of TRAF6 in Central Nervous System. Curr. Neuropharmacol. *16*, 1306–1313. https://doi.org/10.2174/1570159x16666180412094655.
10. Konno, H., Yamamoto, T., Yamazaki, K., Gohda, J., Akiyama, T., Semba, K., Goto, H., Kato, A., Yujiri, T., Imai, T., et al. (2009). TRAF6 Establishes Innate Immune Responses by Activating NF-κB and IRF7 upon Sensing Cytosolic Viral RNA and DNA. PLoS One *4*, e5674. https://doi.org/10.1371/journal.pone.0005674.
11. Youseff, B.H., Brewer, T.G., McNally, K.L., Izuogu, A.O., Lubick, K.J., Presloid, J.B., Alqahtani, S., Chattopadhyay, S., Best, S.M., Hu, X., and Taylor, R.T. (2019). TRAF6 Plays a Proviral Role in Tick-Borne Flavivirus Infection through Interaction with the NS3 Protease. iScience *15*, 489–501. https://doi.org/10.1016/j.isci.2019.05.010.
12. Sharma, N., Verma, R., Kumawat, K.L., Basu, A., and Singh, S.K. (2015). miR-146a suppresses cellular immune response during Japanese encephalitis virus JaOArS982 strain infection in human microglial cells. J. Neuroinflammation *12*, 30. https://doi.org/10.1186/s12974-015-0249-0.
13. Wu, S., He, L., Li, Y., Wang, T., Feng, L., Jiang, L., Zhang, P., and Huang, X. (2013). miR-146a facilitates replication of dengue virus by

dampening interferon induction by targeting TRAF6. J. Infect. *67*, 329–341. https://doi.org/10.1016/j.jinf.2013.05.003.

14. Pu, J., Wu, S., Xie, H., Li, Y., Yang, Z., Wu, X., and Huang, X. (2017). miR-146a Inhibits dengue-virus-induced autophagy by targeting TRAF6. Arch. Virol. *162*, 3645–3659. https://doi.org/10.1007/s00705-017-3516-9.
15. Shukla, A., Rastogi, M., and Singh, S.K. (2021). Zika virus NS1 suppresses the innate immune responses via miR-146a in human microglial cells. Int. J. Biol. Macromol. *193*, 2290–2296. https://doi.org/10.1016/j.ijbiomac.2021.11.061.
16. Zhang, X., Zhu, C., Wang, T., Jiang, H., Ren, Y., Zhang, Q., Wu, K., Liu, F., Liu, Y., and Wu, J. (2017). GP73 represses host innate immune response to promote virus replication by facilitating MAVS and TRAF6 degradation. PLoS Pathog. *13*, e1006321. https://doi.org/10.1371/journal.ppat.1006321.
17. Nowosad, A., Jeannot, P., Callot, C., Creff, J., Perchey, R.T., Joffre, C., Codogno, P., Manenti, S., and Besson, A. (2020). p27 controls Ragulator and mTOR activity in amino acid-deprived cells to regulate the autophagy-lysosomal pathway and coordinate cell cycle and cell growth. Nat. Cell Biol. *22*, 1076–1090. https://doi.org/10.1038/s41556-020-0554-4.
18. Hou, X.-O., Si, J.-M., Ren, H.-G., Chen, D., Wang, H.-F., Ying, Z., Hu, Q.-S., Gao, F., and Wang, G.-H. (2015). Parkin represses 6-hydroxydopamine-induced apoptosis via stabilizing scaffold protein p62 in PC12 cells. Acta Pharmacol. Sin. *36*, 1300–1307. https://doi.org/10.1038/aps.2015.54.
19. Deng, T., Hu, B., Wang, X., Ding, S., Lin, L., Yan, Y., Peng, X., Zheng, X., Liao, M., Jin, Y., et al. (2022). TRAF6 autophagic degradation by avibirnavirus VP3 inhibits antiviral innate immunity via blocking NFKB/NF-κB activation. Autophagy *18*, 2781–2798. https://doi.org/10.1080/15548627.2022.2047384.
20. Liu, J., Li, S., Fei, X., Nan, X., Shen, Y., Xiu, H., Cormier, S.A., Lu, C., Guo, C., Wang, S., et al. (2022). Increased alveolar epithelial TRAF6 via autophagy-dependent TRIM37 degradation mediates particulate matter-induced lung metastasis. Autophagy *18*, 971–989. https://doi.org/10.1080/15548627.2021.1965421.
21. Deng, L., Wang, C., Spencer, E., Yang, L., Braun, A., You, J., Slaughter, C., Pickart, C., and Chen, Z.J. (2000). Activation of the IκB Kinase Complex by TRAF6 Requires a Dimeric Ubiquitin-Conjugating Enzyme Complex and a Unique Polyubiquitin Chain. Cell *103*, 351–361. https://doi.org/10.1016/S0092-8674(00)00126-4.
22. Xia, H., Luo, H., Shan, C., Muruato, A.E., Nunes, B.T.D., Medeiros, D.B.A., Zou, J., Xie, X., Giraldo, M.I., Vasconcelos, P.F.C., et al. (2018). An evolutionary NS1 mutation enhances Zika virus evasion of host interferon induction. Nat. Commun. *9*, 414. https://doi.org/10.1038/s41467-017-02816-2.
23. Zheng, Y., Liu, Q., Wu, Y., Ma, L., Zhang, Z., Liu, T., Jin, S., She, Y., Li, Y.-P., and Cui, J. (2018). Zika virus elicits inflammation to evade antiviral response by cleaving cGAS via NS1-caspase-1 axis. EMBO J. *37*, e99347. https://doi.org/10.15252/embj.201899347.
24. Wu, Y., Liu, Q., Zhou, J., Xie, W., Chen, C., Wang, Z., Yang, H., and Cui, J. (2017). Zika virus evades interferon-mediated antiviral response through the co-operation of multiple nonstructural proteins *in vitro*. Cell Discov. *3*, 17006. https://doi.org/10.1038/celldisc.2017.6.
25. Wu, H., and Arron, J.R. (2003). TRAF6, a molecular bridge spanning adaptive immunity, innate immunity and osteoimmunology. Bioessays *25*, 1096–1105. https://doi.org/10.1002/bies.10352.
26. Lazear, H.M., Govero, J., Smith, A.M., Platt, D.J., Fernandez, E., Miner, J.J., and Diamond, M.S. (2016). A Mouse Model of Zika Virus Pathogenesis. Cell Host Microbe *19*, 720–730. https://doi.org/10.1016/j.chom.2016.03.010.
27. Hu, Y., Dong, X., He, Z., Wu, Y., Zhang, S., Lin, J., Yang, Y., Chen, J., An, S., Yin, Y., et al. (2019). Zika virus antagonizes interferon response in patients and disrupts RIG-I–MAVS interaction through its CARD-TM domains. Cell Biosci. *9*, 46. https://doi.org/10.1186/s13578-019-0308-9.
28. Chaudhary, V., Yuen, K.-S., Chan, J.F.-W., Chan, C.-P., Wang, P.-H., Cai, J.-P., Zhang, S., Liang, M., Kok, K.-H., Chan, C.-P., et al. (2017). Selective Activation of Type II Interferon Signaling by Zika Virus NS5 Protein. J. Virol. *91*, e00163-17. https://doi.org/10.1128/jvi.00163-17.
29. Casanova, J.L., and Abel, L. (2021). Mechanisms of viral inflammation and disease in humans. Science *374*, 1080–1086. https://doi.org/10.1126/science.abj7965.
30. Mladinich, M.C., Conde, J.N., Schutt, W.R., Sohn, S.Y., and Mackow, E.R. (2021). Blockade of Autocrine CCL5 Responses Inhibits Zika Virus Persistence and Spread in Human Brain Microvascular Endothelial Cells. mBio *12*, e0196221. https://doi.org/10.1128/mBio.01962-21.
31. Liu, H., Zhang, L., Sun, J., Chen, W., Li, S., Wang, Q., Yu, H., Xia, Z., Jin, X., and Wang, C. (2017). Endoplasmic Reticulum Protein SCAP Inhibits Dengue Virus NS2B3 Protease by Suppressing Its K27-Linked Polyubiquitylation. J. Virol. *91*, e02234-16. https://doi.org/10.1128/jvi.02234-16.
32. Luo, H., Li, G., Wang, B., Tian, B., Gao, J., Zou, J., Shi, S., Zhu, S., Peng, B.-H., Adam, A., et al. (2020). Peli1 signaling blockade attenuates congenital zika syndrome. PLoS Pathog. *16*, e1008538. https://doi.org/10.1371/journal.ppat.1008538.
33. Shi, J., Liu, Z., and Xu, Q. (2019). Tumor necrosis factor receptor-associated factor 6 contributes to malignant behavior of human cancers through promoting AKT ubiquitination and phosphorylation. Cancer Sci. *110*, 1909–1920. https://doi.org/10.1111/cas.14012.
34. Rutsch, F., MacDougall, M., Lu, C., Buers, I., Mamaeva, O., Nitschke, Y., Rice, G.I., Erlandsen, H., Kehl, H.G., Thiele, H., et al. (2015). A Specific IFIH1 Gain-of-Function Mutation Causes Singleton-Merten Syndrome. Am. J. Hum. Genet. *96*, 275–282. https://doi.org/10.1016/j.ajhg.2014.12.014.
35. Li, T., Qin, J.-J., Yang, X., Ji, Y.-X., Guo, F., Cheng, W.-L., Wu, X., Gong, F.-H., Hong, Y., Zhu, X.-Y., et al. (2017). The Ubiquitin E3 Ligase TRAF6 Exacerbates Ischemic Stroke by Ubiquitinating and Activating Rac1. J. Neurosci. *37*, 12123–12140. https://doi.org/10.1523/jneurosci.1751-17.2017.

STAR★METHODS

KEY RESOURCES TABLE

REAGENT or RESOURCE	SOURCE	IDENTIFIER
Antibodies		
Anti–TRAF6 antibody	Abcam	Cat# ab40675 RRID: AB_778573
Anti–ZIKV NS5 antibody	Gene Tex	Cat# GTX133312 RRID: AB_2750559
Anti-HA tag antibody	Gene Tex	Cat# GTX115044 RRID: AB_10622369
Anti-Flag tag antibody	Sigma	Cat# F1804 RRID: AB_262044
Anti-P62 antibody	Cell Signaling Technology	Cat# 39749S RRID: AB_2799160
Anti-LC3B antibody	Cell Signaling Technology	Cat# 3868S RRID: AB_2137707
Anti-GAPDH antibody	Fude Biotech	Cat# FD0063 RRID: AB_2934268
Rabbit IgG control Polyclonal antibody	Proteintech	Cat# 30000-0-AP RRID: AB_2819035
Anti-Myc tag antibody	Proteintech	Cat# 16286-1-AP RRID: AB_11182162
HRP conjugated goat anti-mouse antibody	Fude Biotech	Cat# FDM007 RRID: AB_2934269
HRP conjugated goat anti-rabbit antibody	Fude Biotech	Cat# FDR007 RRID: AB_213770
Goat Anti-Mouse IgG H&L tagged with Alexa Fluor 488	Abcam	Cat# ab150113 RRID: AB_2576208
Goat Anti-Rabbit IgG H&L tagged with Alexa Fluor 594	Abcam	Cat# ab150080 RRID: AB_2650602
Anti-type I interferon receptor (IFNR) antibody (MAR1-5A3)	Leinco	Cat# I-401 RRID: AB_2491621
Bacterial and virus strains		
Zika Virus (ZIKV)	A gift from Jinchun Zhao, Guangzhou Medical University	KU820898
Chemicals, peptides, and recombinant proteins		
RPMI-1640 Medium	ATCC	Cat# 30–2001
Foetal Bovine Serum (FBS)	CLARK	Cat# FB25015
Penicillin-Streptomycin (P/S)	Gibco	Cat# 15140–122
Dulbecco's Modified Eagle's Medium (DMEM)	Cienry	Cat# CR-12800
Dulbecco's Modified Eagle's Medium (DMEM)	Gibco	Cat# C11995500BT
Dimethyl sulfoxide (DMSO)	Sigma	Cat# D2650
Cycloheximide (CHX)	MedChemExpress	Cat# HY-12320
MG-132	MedChemExpress	Cat# HY-13259
3-Methyladenine (3-MA)	MedChemExpress	Cat# HY-19312
Chloroquine (CQ)	MedChemExpress	Cat# HY-17589A
Z-FA-FMK	MedChemExpress	Cat# HY-P0109A

(*Continued on next page*)

Continued

REAGENT or RESOURCE	SOURCE	IDENTIFIER
C25-140	Selleck	Cat# S6679
TRIzol reagent	Invitrogen	Cat# 15596026
RIPA lysis buffer	Beyotime	Cat# P0013B
PMSF	Selleck	Cat# S3025
PVDF membranes	Merck millipore	Cat# IPVH00010-N1
Bovine Serum Albumin (BSA)	Sigma	Cat# V900933
Phosphate-buffered saline (PBS)	Biosharp	Cat# BL601A
Tween-20	Beyotime	Cat# ST1726
Tanon™ High-sig ECL Western Blotting Substrate	Tanon	Cat# 180-5001
4% formaldehyde	Beyotime	Cat# P0099
Triton X-100	Beyotime	Cat# P0096
Immunol Staining Blocking Buffer	Beyotime	Cat# P0102
Antifade Mounting Medium with DAPI	Beyotime	Cat# P013
RIPA lysis buffer (weak)	Beyotime	Cat# P0013D
protein A+G agarose beads	Beyotime	Cat# P2055
Flag-tagged magnetic beads	Selleck	Cat# B26101
HA-tagged magnetic beads	ThermoFisher	Cat# 88836
NP40	Solarbio	Cat# N8030
Sodium carboxymethyl cellulose	Sigma	Cat# 419311
Crystal violet	Sigma	Cat# C0775
37% formaldehyde	Aladdin	Cat# F111936
Critical commercial assays		
JetPRIME transfection reagent	Polyplus	Cat# 101000046
iScript cDNA synthesis kit	Bio-Rad	Cat# 1708891
iScript SYBR Green One-Step Kit	Bio-Rad	Cat# 1725125
12% SDS-PAGE	Vazyme	Cat# E304
Tanon™ High-sig ECL Western Blotting Substrate	Tanon	Cat# 180-5001
Bio-Plex Pro-Human Cytokine 48-plex Assays	Bio-Rad	Cat# 12007283
Experimental models: Cell lines		
Trophoblast cell line (HTR-8/SVneo)	ATCC	Cat# CRL-3271
Human glioblastoma cell line (U251)	Procell	Cat# CL-0237
Vero cells	ATCC	Cat# CCR-81
HEK293T cells	ATCC	Cat# CRL-11268
Experimental models: Organisms/strains		
Mouse: C57/BL6J	Gempharmatech company	T065274
ZIKV GZ01 strain	provided by Prof. Jincun Zhao, Guangzhou Medical University	GeneBank:KU820898
Oligonucleotides		
Primer: ZiIKV NS5 Forward:	Luo et al.[32]	N/A
Primer: ZiIKV NS5 Reverse:	Luo et al.[32]	N/A
Primer: Human TRAF6 Forward:	Shi et al.[33]	N/A
Primer: Human TRAF6 Reverse:	Shi et al.[33]	N/A
Primer: Human GAPDH Forward:	Luo et al.[32]	N/A

(*Continued on next page*)

Continued

REAGENT or RESOURCE	SOURCE	IDENTIFIER
Primer: Human GAPDH Reverse:	Luo et al.[32]	N/A
Primer: Human IFNβ Forward:	Rutsch et al.[34]	N/A
Primer: Human IFNβ Reverse:	Rutsch et al.[34]	N/A
Primer: Mouse TRAF6 Forward:	Li et al.	N/A
Primer: Mouse TRAF6 Reverse:	Li et al.	N/A
Primer: Mouse GAPDH Forward:	Luo et al.[32]	N/A
Primer: Mouse GAPDH Reverse:	Luo et al.[32]	N/A
Non-Targeting siRNA control	Sangon Biotechnology	N/A
siRNAs targeting TRAF6 mRNA	Liu et al.[20,31]	N/A
siRNAs targeting P62 mRNA	Hou et al.[18]	N/A
Recombinant DNA		
pcDNA vector	Sangon Biotechnology	N/A
Flag-NS1	Sangon Biotechnology	NCBI: YP_009430301
Flag-NS2A	Sangon Biotechnology	NCBI: YP_009430302
Flag-NS2B	Sangon Biotechnology	NCBI: YP_009430303
Flag-NS3	Sangon Biotechnology	NCBI: YP_009430304
Flag-NS4A	Sangon Biotechnology	NCBI: YP_009430305
Flag-NS4B	Sangon Biotechnology	NCBI: YP_009430307
Flag-NS5	Sangon Biotechnology	NCBI: YP_009430308
HA-TRAF6	Sangon Biotechnology	NCBI: NM_004620
Myc-K63	Gift from Prof. Yuelong Shu, Sun Yat-sen University	N/A
Myc-K48	Gift from Prof. Yuelong Shu, Sun Yat-sen University	N/A
Software and algorithms		
Graphpad Prism 8	Graphpad software	https://www.graphpad.com
Image J	Fiji software	https://imagej.net/software/fiji/
CFX96 real-time PCR system	Bio-Rad	https://www.bio-rad.com/
Chemiluminescence imaging system	SageCreation	http://www.sagecreation.com.cn/en/
All-in-One Fluorescence Microscope BZ-X800	KEYENCE	https://www.keyence.com/
Bio-Plex 200 systems	Bio-Rad	https://www.bio-rad.com/

EXPERIMENTAL MODEL AND STUDY PARTICIPANT DETAILS

Animal experiments

Wild-type (WT) C57BL/6 mice (both male and female, aged 6-8 weeks) were purchased from the Gempharmatech company. The mice were treated with 2 mg MAR1-5A3 on the day prior to infection and then intraperitoneally inoculated with 5×10^4 plaque-forming units (PFU) of ZIKV GZ01 or an equivalent volume of PBS. Tissues were harvested on day 2 and day 6 upon ZIKV infection. The experiment with infectious ZIKV were conducted under biosafety level 2 (BSL2) facilities at School of Public Health, Shenzhen (Sun Yat-sen University, China) and Beijing Laboratory Animal Research Center. The animal experiments were approved by the Animal Care and Use Committee of Sun Yat-sen University.

Cell culture and virus

The trophoblast cell line (HTR-8/SVneo) was obtained from the American Type Culture Collection (ATCC, CRL-3271) and cultured in RPMI-1640 medium (ATCC) containing 5% foetal bovine serum (FBS; CLARK) and 1% Penicillin-Streptomycin (P/S, Gibco). The human glioblastoma cell line (U251) was purchased by Procell Life Science & Technology Co., Ltd (Procell) and maintained in high-glucose Dulbecco's modified Eagle's medium (DMEM; Cienry) containing 10% FBS and 100 units/ml Penicillin-Streptomycin. The African green monkey (Vero) cell line (ATCC) was provided by Prof. Caijun Sun from Sun Yat-sen University and cultured in Dulbecco's modified Eagle's medium (DMEM; Gibco) containing 10% FBS and 100 units/ml Penicillin-Streptomycin. HEK293T cell line (ATCC) was provided by Prof. Yuelong Shu from Sun Yat-sen

University and cultured in Dulbecco's modified Eagle's medium (DMEM; Gibco) containing 10% FBS and 100 units/ml Penicillin-Streptomycin. All cells were cultured at 37°C in a 5% CO2 atmosphere.

The Asian lineage ZIKV GZ01 strain ((GeneBank: KU820898)) used in this study was provided by Prof. Jincun Zhao from Guangzhou Medical University.

METHOD DETAILS

Viral infection

HTR8 cells, and U251 cells were washed with PBS and infected with ZIKV GZ01 at a multiplicity of infection (MOI) of 1 or non-infected group in culture medium. The cells were incubated with the virus for 1 hour with intermittent shaking every 20 min. Cell samples were collected at different time points for analysis.

Viral titres were determined by performing a plaque assay on Vero cells. For plaque assay, Vero cells were seeded at the confluence in 24-well tissue culture plates. Serial dilutions of culture supernatants were prepared in DMEM (Gibco) containing 2% FBS and added to the cells for 1 hours. The virus media was removed, and an equal mixture of Sodium carboxymethyl cellulose containing 2% FBS was added onto the monolayer and incubated for 4 days (at 37°C in a 5% CO2 atmosphere). The cell monolayer was fixed with 3.7% formaldehyde (Aladdin) for 30 min followed by careful removal of the solution and the overlay media. The cells were stained using a 1% crystal violet (Sigma) solution for 1 min and washed with distilled water to visualize the plaques.

Proteomic analysis

Total cellular protein extracted from ZIKV-infected HTR8 cells and non-infected cells was examined with data-independent acquisition (DIA) proteomics by BGI Genomics (Shenzhen, Guangdong, China). Differential expression analysis was used to identify the potential downregulated proteins after ZIKV-infected.

Quantitative real-time PCR (qPCR)

Total intracellular RNA was isolated using the TRIzol reagent (Invitrogen). The isolated RNA was then converted to complementary DNA (cDNA) using the iScript cDNA synthesis kit (Bio-Rad), following the manufacturer's protocol. The qPCR was performed in the CFX96 real-time PCR system (Bio-Rad) with iScript SYBR Green One-Step Kit (Bio-Rad). All primers were synthesized by Sangon Biotechnology (Shanghai, China). The primers used for RT-qPCR were as follows:

ZIKV NS5 Forward: 5'-GGTCAGCGTCCTCTCTAATAAACG-3'[32]
ZIKV NS5 Reverse: 5'-GCACCCTAGTGTCCACTTTTTCC-3'[32]
Human TRAF6 Forward: 5'-ATGCGGCCATAGGTTCTGC-3'[33]
Human TRAF6 Reverse: 5'-TCCTCAAGATGTCTCAGTTCCAT-3'[33]
Human GAPDH Forward: 5'-CTGACTTCAACAGCGACACC-3'[32]
Human GAPDH Reverse: 5'-TAGCCAAATTCGTTGTCATACC-3'[32]
Human IFNβ Forward: 5'-ATTGCTCTCCTGTTGTGCTT-3'[34]
Human IFNβ Reverse: 5'-TCTCCTCAGGGATGTCAAAGT-3'[34]
Mouse TRAF6 Forward: 5'-CTGAAAGGGTGGCAACTTCT-3'[35]
Mouse TRAF6 Reverse: 5'-CTGGCACTTCTGGAAAGGAC-3'[35]
Mouse GAPDH Forward: 5'-AGGTCGGTGTGAACGGATTTG-3'[32]
Mouse GAPDH Reverse: 5'-TGTAGACCATGTAGTTGAGGTCA-3'[32]

Western blot

At different time points, proteins were harvested from cells and animal tissues and lysed in RIPA lysis buffer (Beyotime) containing 1% PMSF (Selleck). Protein samples were prepared and separated on 12% SDS-PAGE (Vazyme), followed by transfer to PVDF membranes (Merck millipore). After blocking with 5% bovine serum albumin (BSA; Sigma) in phosphate-buffered saline (PBS; Biosharp) containing 0.05% Tween-20 (Beyotime) for 1 hour at room temperature (RT), the membranes were washed three times with PBS containing 0.05% Tween-20, and then incubated with the indicated primary antibodies overnight at 4°C. Next day, the blots were incubated with secondary antibodies. Protein bands were then visualized using Tanon™ High-sig ECL Western Blotting Substrate (Tanon) and imaged using Chemiluminescence imaging system (SAGECREATION, MiniChemi610).

Immunofluorescence assay

The cells were fixed with 4% formaldehyde (Beyotime) for 15 minutes and then permeabilized with Triton X-100 (Beyotime) for 5 minutes at RT. Next, cells were blocked in Immunol Staining Blocking Buffer (Beyotime) for 1 hour at RT, followed by overnight incubation at 4°C with primary antibodies diluted in PBS containing 3% BSA. After three washing steps with PBS containing 0.5% Tween-20, the cells were incubated for 1 hour with secondary antibodies: Goat Anti-Mouse IgG H&L tagged with Alexa Fluor 488 (Abcam) and Goat Anti-Rabbit IgG H&L tagged with Alexa Fluor 594 (Abcam). Thereafter, cells were washed with PBS containing 0.5% Tween-20 and mounted in Antifade Mounting Medium with DAPI (Beyotime). Images were captured using the All-in-One Fluorescence Microscope BZ-X800 (KEYENCE).

Co-immunoprecipitation (Co-IP)

U251 cells or HEK293T cells containing plasmids were lysed in RIPA lysis buffer (weak) (Beyotime) containing 1% PMSF (Selleck). Cell lysates were centrifuged at 12000 × g for 20 min at 4°C, and the supernatant was incubated with protein A+G agarose beads (Beyotime), Flag-tagged magnetic beads (Selleck) or HA-tagged magnetic beads (ThermoFisher) at 4°C for 12-14 hours. Then the beads were washed with TBST (Beyotime) containing 1% NP40 (Solarbio) and 0.5% Tween-20 for three times and resolved with protein loading buffer. The target proteins were detected by western blot. In Figures 5H and 5I, 293T cells were co-transfected with Myc-K63 (5 μg) plasmid (Figure 5H) or Myc-K48 (5 μg) plasmid (Figure 5I), Flag-NS1 (5 μg) and HA-TRAF6 (5 μg) plasmids for 48h. HEK293T cells containing plasmids were lysed in RIPA lysis buffer (weak) (Beyotime) containing 1% PMSF (Selleck). Cell lysates were centrifuged at 12000 × g for 20 min at 4°C, and the supernatant was incubated with anti-Flag magnetic beads at 4°C for 12-14 hours. Then the beads were washed with TBST (Beyotime) containing 1% NP40 (Solarbio) and 0.5% Tween-20 for three times and resolved with protein loading buffer. The target proteins were detected by western blot as described previously.

Cytokine Bio-Plex assay

Cell culture supernatants were collected for analysis of cytokine production using Bio-Plex Pro-Human Cytokine 48-plex Assays (Bio-Rad). The levels of cytokines were analyzed with the Bio-Plex 200 systems (Bio-Rad), following the manufacturer's instructions.

QUANTIFICATION AND STATISTICAL ANALYSIS

All data were analyzed using GraphPad Prism software (version 8). The results are presented as means ± standard deviation (SD). Statistical significance is determined either unpaired Student's *t* test or one-way ANOVA with Tukey test for multiple comparisons. ns indicates a non-significant difference. *P*-values are indicated as follows: * $P< 0.05$, ** $P< 0.01$, *** $P< 0.001$, and **** $P < 0.0001$.